J|A|C|S COMMUNICATIONS

Published on Web 12/16/2009

Highly Permeable Zeolite Imidazolate Framework-8 Membranes for CO_2/CH_4 Separation

Surendar R. Venna and Moises A. Carreon*

Department of Chemical Engineering, University of Louisville, Louisville, KY-40292

Received October 31, 2009; E-mail: macarr15@louisville.edu

From the environmental and energy perspective, purification and recovery of carbon dioxide from flue gas and natural gas are of great interest. CO_2 is the main component of the greenhouse gases, and its accumulation in the environment is leading to severe global warming issues. World CO_2 emissions in 2005 were estimated at 28 051 million metric tons (MMT) and projected to 42 325 MMT for 2030.[1] To alleviate CO_2 accumulation it is important to separate and recycle CO_2 before it is released to air. Moreover, CO_2 is an undesirable impurity in natural gas wells, with concentrations as high as 70%.[2] CO_2 must be separated from CH_4 because it reduces the energy content of the natural gas, and it is acidic and corrosive in the presence of water. Removing CO_2 without large energy expenditures is desirable, and thus membranes that preferentially permeate CO_2 at high selectivities can significantly impact utilization of these gas wells by reducing the costs of natural gas purification.[2] Polymeric membranes such as cellulose acetate, polymide and polyramide,[3] and highly branched poly(ethylene oxide)[4] can separate CO_2 from CH_4. However, due to its superior thermal, mechanical, and chemical stability and good erosion resistance, zeolite membranes such as SAPO-34,[5] Linde type T,[6] silicalite-1,[7] and DD3R[8] are preferred over polymeric membranes for CO_2 separation from CH_4.

Zeolite imidazolate frameworks (ZIFs),[9] a subclass of metal organic frameworks (MOFs), have emerged as a novel type of crystalline porous material which combine highly desirable properties from both zeolites and MOFs, such as microporosity, high surface areas, and exceptional thermal and chemical stability, making them ideal candidates for gas separation applications. The potential of MOFs as membranes has been recognized by extensive modeling studies.[10] These models have given useful insights into the kinds of pore structures that are desirable for gas separations and suggest ZIFs as one of these desirable compositions. In ZIFs, metal atoms such as Zn, Co, and Cu are linked through N atoms by ditopic imidazolate (Im) or functionalized Im links to form neutral frameworks and to provide tunable nanosized pores formed by four, six, eight, and twelve membered ring ZnN_4, CoN_4, and CuN_4 tetrahedral clusters.[9d] The framework of ZIF compounds closely resembles the framework of zeolites; i.e., the T−O−T bridges (T = Si, Al, P) in zeolites are replaced by M−Im−M bridges (M = Zn, Co, Cu), and coincidentally, their bond angles in both structures are 145°.[9c]

In particular, ZIF-8 is one of the most studied prototypical ZIF compounds,[9a,b,g,11] due to its potential functional applications in gas storage (CO_2, H_2, and acetylene), catalysis, and gas separations. ZIF-8 has large pores of 11.6 Å which are accessible through small apertures of 3.4 Å, and it has a cubic space group (I-43*m*) with unit cell dimensions of 16.32 Å. It has the sodalite (SOD) zeolite-type structure with approximately two times larger pore sizes than those of the corresponding SOD zeolites.[11a,b,e] Due to its highly porous open framework structure, large accessible pore volume with fully exposed edges and faces of the organic links, pore apertures in the range of the kinetic diameter of several gas molecules, and high CO_2 adsorption capacity, ZIF-8 is highly attractive for gas separation applications. Furthermore, it has been demonstrated that ZIF-8 is chemically stable in the presence of water and some aromatic hydrocarbons such as benzene,[9b] which are typical impurities in natural gas, making this particular ZIF composition potentially useful for the separation of CO_2 from CH_4. Thermally and chemically stable ZIF-8 particles have been synthesized by solvothermal methods and synthesis times between 1 h and 1 month[9a,b,g] employing diverse gel compositions and synthesis conditions. ZIF-8 crystals with a narrow particle size distribution and sizes from micrometers (∼150 μm)[9b] to nanometers (∼50 nm)[9g] and surface areas in the 900−1600 m^2/g[9g,b] range have been prepared.

Few examples on MOF-polymer composite membranes[12] and pure MOF membrane[13] compositions for gas separations have been reported. Recently, ZIF-8-polymer composite membranes have been used for liquid phase separations.[14] However, there is no report on any *pure* thin ZIF membrane composition. Herein, we report the synthesis, characterization, and CO_2/CH_4 gas separation performance of tubular alumina supported ZIF-8 membranes. To the best of our knowledge, this is the first example of the preparation of thin, continuous and reproducible ZIF-8 membranes for a functional gas separation application. The synthesized ZIF-8 membranes displayed unprecedented high CO_2 permeances and relatively high separation indexes for equimolar mixtures of CO_2 and CH_4.

The XRD pattern of the hydrothermal synthesized ZIF-8 seeds is shown in Figure 1a. The XRD pattern corresponds to the SOD structure, which is the typical structure of ZIF-8. The relative intensity and peak positions of the XRD pattern are in agreement with previous reports,[9b,g] confirming the formation of pure crystalline ZIF-8 phase. The interplanar spacings calculated using Bragg's law from the reflections at different Bragg's angles presented in Table S1[15] are in good agreement with previous literature.[9b,g] The average crystal size was ∼45 nm, calculated using Scherrer's equation from the broadening of the XRD peaks. The formation of ZIF-8 was confirmed by a TEM diffractogram, as shown in Figure 1b. The diffraction rings of the different planes, shown in Figure 1b, are in good agreement with the XRD peaks of ZIF-8 as shown in Table S1[15] and correspond to a body centered cubic structure with a unit cell parameter of 16.48 Å. Absorption FTIR spectra (Figure S2) revealed the typical lattice vibration frequencies of the ZIF-8 structure.[15] The morphological features of ZIF-8 crystals were inspected under TEM (Figure 1c). Sharp hexagonal faceted and homogeneous ∼55 nm crystals were observed. A magnified image of the TEM of the hexagonal-like particles reveals the spacing of the lattice fringes matching with the *d*-spacing of the (2 2 2) planes (Figure 1d). These lattice fringes were taken with minimum TEM beam exposure time because of the fast amorphization of the crystals. The CHN analysis revealed the carbon, hydrogen, and nitrogen contents in the ZIF-8 framework, C - 41.7%, H - 4.5%,

10.1021/ja909263x

and N - 24.4% (ash ~ 29.4%), which are in good agreement with the calculated theoretical amounts (C - 42.2%, H - 4.4%, and N - 24.6%).[9g]

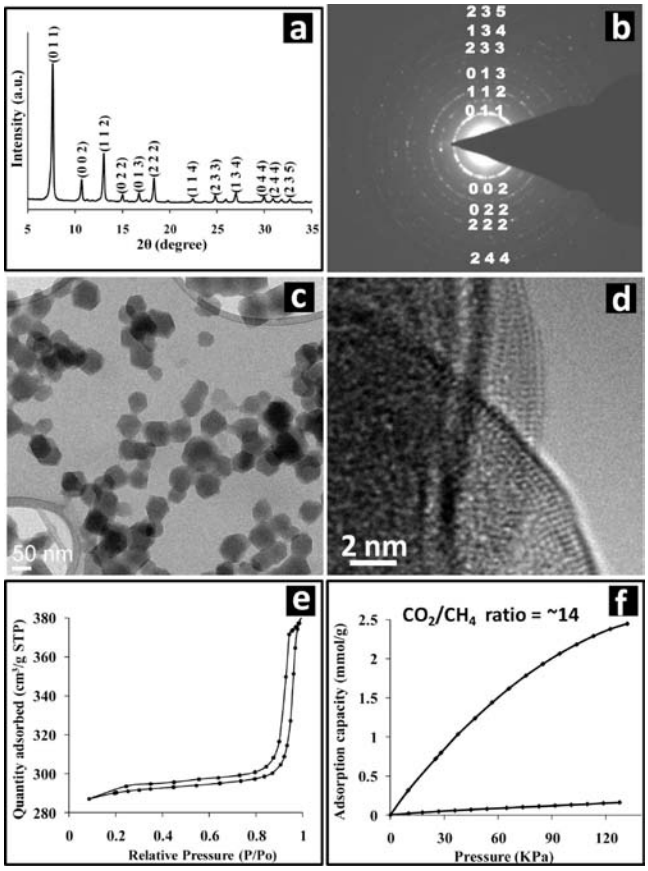

Figure 1. ZIF-8 seeds employed for membrane synthesis: (a) XRD pattern; (b) Diffraction pattern; (c) TEM image; (d) Magnified image of the TEM; (e) Nitrogen adsorption−desorption isotherm; and (f) CO_2 and CH_4 adsorption isotherms.

The apparent surface area and micropore volume of the ZIF-8 nanocrystals were 1072 m^2/g and 0.53 cm^3/g respectively, using BET and DR methods and taking the data points on the nitrogen branch in the range of P/P_0 of 0.01− 0.3. Type I isotherms (Figure 1e) were observed indicating the microporous nature of the ZIF-8 crystals. The adsorption isotherms of CO_2 and CH_4 on ZIF-8 were collected at room temperature using water as the coolant. The ZIF-8 crystals adsorbed CO_2 preferentially over CH_4. At 100 KPa, the ZIF-8 crystals adsorbed ~14 times more CO_2 than CH_4 as shown in Figure 1f. Although CO_2 is a nonpolar molecular, the polar nature of its carbon−oxygen bonds may favor its binding and preferential adsorption on polar ZIF-8 walls.[9c] The preferential adsorption of CO_2 over CH_4 makes ZIF-8 crystals highly attractive for CO_2 purification from natural gas.

ZIF-8 membranes were synthesized by in situ crystallization on tubular porous α-alumina supports. The hydrothermal synthesized seeds provided nucleation sites for membrane growth. CO_2/CH_4 separation performance of the alumina supported ZIF-8 membranes is shown in Table 1. All membranes were coated with two layers except Z4, which was coated with eight layers. The thickness of the two layer membrane was ~5 μm as shown in Figure 2a, while the eight layer membrane was ~9 μm thick (Figure 2b). The small thickness difference between the two layered and eight layered membranes suggests partial dissolution of the first layers. ZIF-8 crystals of ~110 ± 15 nm allowed the formation of continuous thin membranes as shown in Figure 2c. The size of the well-defined spherical-like crystals on the membrane increased considerably as compared to the size of the seed crystals (Figure 1c). This increase in crystal size may be related to the recrystallization and sintering of the crystals with the incorporation of the ZIF-8 layers. It is important to mention that although TEM images show the presence of well-defined hexagonal crystals for ZIF-8 seeds (Figure 1c), SEM images (Figure S3)[15] revealed spherical-like particles of similar size. The prolonged exposure time of the SEM electron beam

Table 1. CO_2/CH_4 Separation Properties of ZIF-8 Membranes at a Permeate Pressure of 99.5 KPa and Pressure Drop of 40 KPa

membrane ID[a]	P_{CO_2} mol/m²·s·Pa (×10⁵)	P_{CH_4} mol/m²·s·Pa (×10⁶)	CO_2/CH_4 selectivity	separation index (π)[b]
Z1	2.43	4.72	5.1	9.9
Z2	2.19	4.63	4.7	8.0
Z3	2.11	5.17	4.1	6.5
Z4	1.69	2.42	7.0	10.0

[a] Z1−Z3 are 2 layered membranes; Z4 is 8 layered membrane. [b] $\pi = (P_{CO_2} \times (\text{selectivity-1})) \times$ Permeate pressure.[5e]

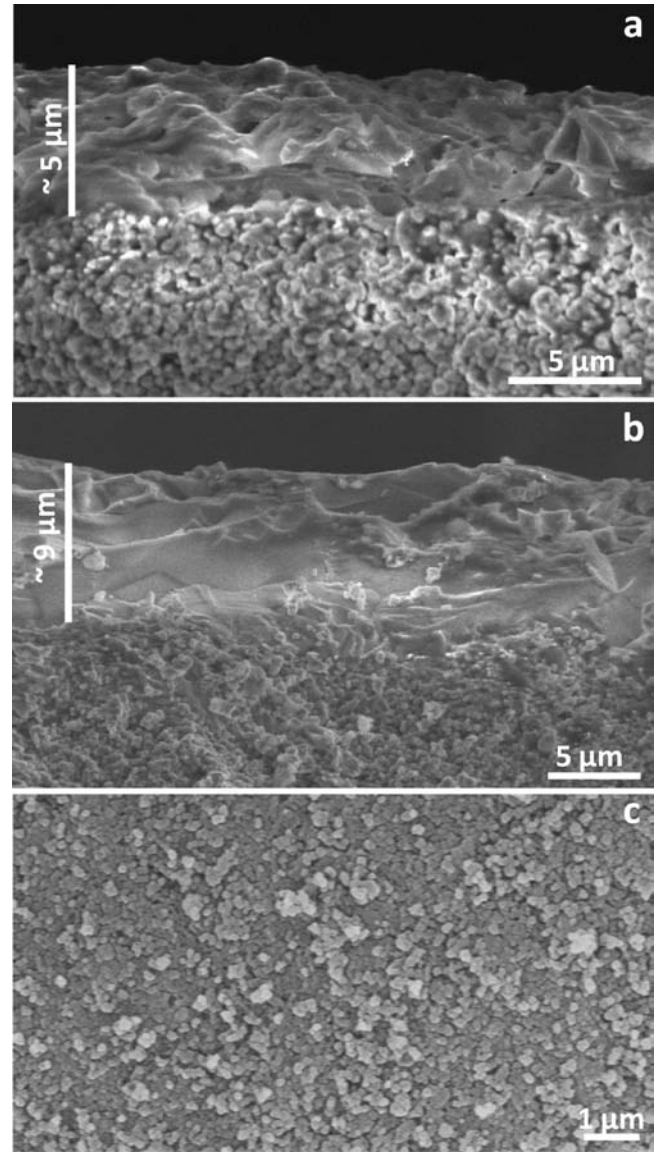

Figure 2. ZIF-8 membranes: cross-sectional view of (a) two layer and (b) eight layer membranes and (c) top view of the two layer membrane.

promoted the amorphization of the hexagonal-like crystals to a spherical-like morphology. In fact, a detailed inspection of Figure 1c reveals that even with minimum TEM exposure time, some hexagonal crystals transformed to spherical shapes as a result of surface energy minimization, a phenomenon well-known as roughening transition.[16] The XRD patterns of the membranes corresponded to the ZIF-8 structure.[15]

ZIF-8 membranes displayed unprecedented high CO_2 permeances up to $\sim 2.4 \times 10^{-5}$ mol/m^2·s·Pa and CO_2/CH_4 selectivities from ~4 to 7 at 295 K and a feed pressure of 139.5 KPa, the maximum pressure that the membranes could hold. The separation index of the membranes ranged from ~6.5 to 10, which is comparable with that of some alumina supported SAPO-34 membranes.[5d] The addition of multiple layers in sample Z4 increased the CO_2/CH_4 selectivity and decreased the CO_2 permeance, most likely due to the reduction of nonzeolite pores and increase in membrane thickness respectively (Table 1). The high observed CO_2 permeances were associated not only due to the presence of small crystals with a narrow size distribution, which led to thin membranes, but also due to the textural properties of the alumina porous support which is composed of an outer layer of 0.2 μm average pore size and a porous area of 0.8 μm average pore size. The outer layer provided a smoother surface for uniform intergrowth of the ZIF-8 crystals with the support surface, while the porous area of 0.8 μm average pore size translated into higher fluxes. The CO_2/CH_4 selectivity of the membranes was low, most likely due to a high concentration of nonzeolite pores. Despite the low CO_2/CH_4 selectivity, the high CO_2 permeances contributed to the relatively high separation indexes. Although ZIF-8 is composed of large 11.6 Å pores and small pore apertures of 3.4 Å, density functional theory simulation data suggest that the smaller pores are the preferential adsorption sites for CO_2 molecules.[17] Therefore, the small pore aperture of ZIF-8 may favor the diffusion of CO_2 (kinetic diameter $\approx$ 3.3 Å) over CH_4 (kinetic diameter $\approx$ 3.8 Å).

In summary, reproducible thin ZIF-8 membranes with an ~5−9 μm thickness were synthesized by secondary seeded growth on tubular α-Al_2O_3 porous supports. The separation performance of these membranes for equimolar CO_2/CH_4 gas mixtures was demonstrated. The membranes displayed unprecedented CO_2 permeances as high as $\sim 2.4 \times 10^{-5}$ mol/m^2·s·Pa with CO_2/CH_4 separation selectivities of ~4 to 7 and separation indexes in the ~6.5 to 10 range at 295 K and a feed pressure of 139.5 KPa. Currently, we are exploring diverse chemical (compositions, reagents nature) and processing (number of layers, hydrothermal synthesis time and temperature) parameters to prepare more robust and more selective membranes able to hold higher feed pressures for CO_2/CH_4 separation.

Acknowledgment. This work was partially supported by an ACS-PRF grant. We thank Dr. Jacek B. Jasinski, IAMRE, University of Louisville, for his invaluable help in TEM experiments.

Supporting Information Available: Experimental Procedure, Calculations of *d*-spacing and matching with TEM diffractogram, FT-IR, Gas separation system, SEM image of ZIF-8 seeds, XRD pattern of the membrane. This material is available free of charge via the Internet at http://pubs.acs.org.

References

(1) Department of Energy; *Annual Energy Outlook*; Report # DOE/EIA 0383; June 2008.
(2) Lin, H.; Van Wagner, E.; Raharjo, R.; Freeman, B. D.; Roman, I. *Adv. Mater.* **2006**, *18*, 39.
(3) Koros, W. J.; Mahajan, R. *J. Membr. Sci.* **2000**, *175*, 181.
(4) Lin, H.; Van Wagner, E.; Freeman, B. D.; Toy, L. G.; Gupta, R. P. *Science* **2006**, *311*, 639.
(5) (a) Poshusta, J. C.; Tuan, V. A.; Pape, E. A.; Noble, R. D.; Falconer, J. L. *AIChE J.* **2000**, *46*, 779. (b) Li, S.; Falconer, J. L.; Noble, R. D. *J. Membr. Sci.* **2004**, *241*, 121. (c) Li, S.; Falconer, J. L.; Noble, R. D. *Adv. Mater.* **2006**, *18*, 2601. (d) Carreon, M. A.; Li, S.; Falconer, J. L.; Noble, R. D. *J. Am. Chem. Soc.* **2008**, *130*, 5412. (e) Carreon, M. A.; Li, S.; Falconer, J. L.; Noble, R. D. *Adv. Mater.* **2008**, *20*, 729.
(6) Cui, Y.; Kita, H.; Okamoto, K. I. *J. Mater. Chem.* **2004**, *14*, 924.
(7) Guo, H.; Zhu, G.; Li, H.; Zou, X.; Yin, X.; Yang, W.; Qiu, S.; Xu, R. *Angew. Chem., Int. Ed.* **2006**, *45*, 7053.
(8) (a) Tomita, T.; Nakayama, K.; Sakai, H. *Microporous Mesoporous Mater.* **2004**, *68*, 71. (b) Van den Bergh, J.; Zhu, W.; Gascon, J.; Moulijn, J. A.; Kapteijn, F. *J. Membr. Sci.* **2008**, *316*, 35.
(9) (a) Huang, X.-C.; Lin, Y.-Y.; Zhang, J. P.; Chen, X.-M. *Angew. Chem., Int. Ed.* **2006**, *45*, 1557. (b) Park, K. S.; Ni, Z.; Cote, A. P.; Choi, J. Y.; Huang, R.; Uribe-Romo, F. K.; Chae, H. K.; O'Keeffe, M.; Yaghi, O. M. *Proc. Natl. Acad. Sci. U.S.A.* **2006**, *103*, 10186. (c) Hayashi, H.; Côté, A. P.; Furukawa, H.; O'Keeffe, M.; Yaghi, O. M. *Nat. Mater.* **2007**, *6*, 501. (d) Banerjee, R.; Phan, A.; Wang, B.; Knobler, C.; Furukawa, H.; O'Keeffe, M. *Science* **2008**, *319*, 939. (e) Wang, B.; Côté, A. P.; Furukawa, H.; O'Keeffe, M.; Yaghi, O. M. *Nature* **2008**, *453*, 207. (f) Morris, W.; Doonan, C. J.; Furukawa, H.; Banerjee, R.; Yaghi, O. M. *J. Am. Chem. Soc.* **2008**, *130*, 12626. (g) Cravillon, J.; Muzer, S.; Lohmeier, S. J.; Feldhoff, A.; Huber, K.; Wiebcke, M. *Chem. Mater.* **2009**, *21*, 1410. (h) Banerjee, R.; Furukawa, H.; Britt, D.; Knobler, C.; O'Keeffe, M.; Yaghi, O. M. *J. Am. Chem. Soc.* **2009**, *131*, 3875.
(10) (a) Keskin, S.; Sholl, D. S. *Ind. Eng. Chem. Res.* **2009**, *48*, 914. (b) Keskin, S.; Sholl, D. S. *Langmuir* **2009**, *25*, 11786. (c) Keskin, S.; Sholl, D. S. *J. Phys. Chem. B* **2007**, *111*, 14055. (d) Keskin, S.; Liu, J.; Rankin, R. B.; Johnson, J. K.; Sholl, D. S. *Ind. Eng. Chem. Res.* **2009**, *48*, 2355. (e) Watanabe, T.; Keskin, S.; Nair, S.; Sholl, D. S. *Phys. Chem. Chem. Phys.* **2009**, *11*, 11389.
(11) (a) Wu, H.; Zhou, W.; Yildrim, T. *J. Am. Chem. Soc.* **2007**, *129*, 5314. (b) Zhou, W.; Wu, H.; Udovic, T. J.; Rush, J. J.; Yildrim, T. *J. Phys. Chem. A* **2008**, *112*, 12602. (c) Jiang, H. L.; Liu, B.; Akita, T.; Haruta, M.; Sakurai, H.; Xu, Q. *J. Am. Chem. Soc.* **2009**, *131*, 11302. (d) Moggach, S. A.; Bennett, T. D.; Cheetham, A. K. *Angew. Chem., Int. Ed.* **2009**, *48*, 1. (e) Wu, H.; Zhou, W.; Yildrim, T. *J. Phys. Chem. C* **2009**, *113*, 3029. (f) Xiang, S.; Zhou, W.; Gallegos, J. M.; Liu, Y.; Chen, B. *J. Am. Chem. Soc.* **2009**, *131*, 12415.
(12) (a) Zhang, Y.; Musselman, I. H.; Ferraris, J. P.; Balkus, K. J. *J. Membr. Sci.* **2008**, *313*, 170. (b) Perez, E. V.; Balkus, K. J.; Ferraris, J. P.; Musselman, I. H. *J. Membr. Sci.* **2009**, *328*, 165.
(13) (a) Ranjan, R.; Tsapatsis, M. *Chem. Mater.* **2009**, *21*, 4920. (b) Gascon, J.; Aguado, S.; Kapteijn, F. *Microporous Mesoporous Mater.* **2008**, *113*, 132. (c) Liu, Y.; Ng, Z.; Khan, E. A.; Jeong, H.-K.; Ching, C.-B.; Lai, Z. *Microporous Mesoporous Mater.* **2009**, *118*, 296. (d) Guo, H.; Zhu, G.; Hewitt, I. J.; Qiu, S. *J. Am. Chem. Soc.* **2009**, *139*, 1646.
(14) Basu, S.; Maes, M.; Cano-Odena, A.; Alaerts, L.; De Vos, D. E.; Vankelecom, I. F. J. *J. Membr. Sci.* **2009**, *344*, 190.
(15) See Supporting Information
(16) (a) Vogels, L. J. P.; van Hoof, P. J. C. M.; Grimbergen, R. F. P. *J. Cryst. Growth* **1998**, *191*, 563. (b) Cundy, C. S.; Henty, M. S.; Plaisted, R. J. *Zeolites* **1995**, *15*, 353.
(17) Liu, D.; Zheng, C.; Yang, Q.; Zhong, C. *J. Phys. Chem. C* **2009**, *113*, 5004.

JA909263X